Bioorganic & Medicinal Chemistry 16 (2008) 6601–6610

Contents lists available at ScienceDirect

Bioorganic & Medicinal Chemistry

journal homepage: www.elsevier.com/locate/bmc

# In vitro and in vivo anti-tumoral activities of imidazo[1,2-*a*]quinoxaline, imidazo[1,5-*a*]quinoxaline, and pyrazolo[1,5-*a*]quinoxaline derivatives

Georges Moarbess [a,†], Carine Deleuze-Masquefa [a,*,†], Vanessa Bonnard [a], Stéphanie Gayraud-Paniagua [a], Jean-Rémi Vidal [c], Françoise Bressolle [b,c], Frédéric Pinguet [c], Pierre-Antoine Bonnet [a]

[a] *Laboratoire de Pharmacochimie et Biomolécules, EA 4215, Faculté de Pharmacie, Université Montpellier I, 15 av. Charles Flahault, BP 14491, 34 093 Montpellier Cedex 5, France*
[b] *Laboratoire de Pharmacocinétique Clinique, EA 4215, Faculté de Pharmacie, Université Montpellier I, 15 av. Charles Flahault, BP 14491, 34 093 Montpellier Cedex 5, France*
[c] *Centre Régional de Lutte contre le Cancer, Val d'Aurelle, Rue de la Croix Verte, 34000 Montpellier, France*

ARTICLE INFO

*Article history:*
Received 5 February 2008
Revised 2 May 2008
Accepted 7 May 2008
Available online 10 May 2008

*Keywords:*
Imidazoquinoxalines
Pyrazoloquinoxaline
Imiquimod
Melanoma
In vitro activity
Pharmacodynamic evaluation

ABSTRACT

Imidazoquinoxaline and pyrazoloquinoxaline derivatives, analogues of imiquimod, were synthesized, and their in vitro cytotoxic and pharmacodynamic activities were evaluated. In vitro cytotoxicity studies were assessed against melanoma (A375, M4Be, RPMI-7591), colon (LS174T), breast (MCF7), and lymphoma (Raji) human cancer cell lines. In vivo studies were carried out in M4Be xenografted athymic mice. **EAPB0103**, **EAPB0201**, **EAPB0202**, and **EAPB0203** showed significant in vitro activities against A375 compared to fotemustine and imiquimod used as references. These compounds were 6–110 and 2–45 times more active than fotemustine and imiquimod, respectively. **EAPB0203** bearing phenethyl as substituent at position 1 and methylamine at position 4 showed the highest activity. **EAPB0203** has also a more potent cytotoxic activity than imiquimod and fotemustine in M4Be and RPMI-7591 and interesting cytotoxic activity in other tumor cell lines tested. In vivo, **EAPB0203** treatment schedules caused a significant decrease in tumor size compared to vehicle control and fotemustine treatments.



## 1. Introduction

Imiquimod, an imidazoquinoline amine, is an immunomodulating agent approved in 1997 by the U.S Food and Drugs Administration for treating external genital and peri-anal warts.[1–3] In murine animal models, imiquimod has proven its efficacy in a variety of transplantable tumors including colon carcinomas, melanomas, lung sarcomas, mammary, and bladder carcinomas.[2] It has shown activities toward basal cell carcinomas (BCC),[3,4] actinic keratoses,[4,5] and some melanoma metastases,[6–9], and its therapeutic spectrum was extended to cutaneous B-cell lymphomas.[10]

Extensive studies over the past years indicated that imiquimod acts both: (i) indirectly, by activating the innate as well as the adaptive immune system via binding to cell surface receptors such as Toll-like receptors (TLR) 7 and 8, thereby inducing the activation of transcription factors like nuclear factor NF-κB and resulting in the secretion of pro-inflammatory cytokines predominantly interferon (IFN)-α, tumor necrosis factor (TNF)-α and interleukin (IL)-12,[11,12] and (ii) directly, by inducing direct in vitro and in vivo pro-apoptotic activities in a rather tumor selective manner,[11,13,14] requiring the activation of the 'work horses' of apoptosis, the caspases' family of proteases.

Responsible of several thousand deaths each year, melanoma is the most frequent malignant tumor in the white human population worldwide. Its frequency increases dramatically with age and chronic sun exposure. INF-α, IL-2, some chemotherapeutic drugs, and tumor-directed vaccination have been evaluated in clinical trials. All of these approaches, unfortunately, met with rather limited success. Given the limited effectiveness of a large variety of conventional anti-cancer drugs in the treatment of melanoma such as various chemo-and/or immunotherapies, novel approaches or drugs selectively targeting melanoma cells are urgently needed.

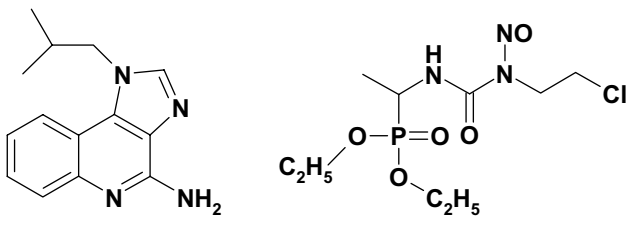


imiquimod fotemustine

**Figure 1.** Chemical structures of imiquimod and fotemustine.

* Corresponding author. Tel: +33 4 67548665/8640; fax.: +33 4 67548036.
*E-mail address:* carine.masquefa@univ-montp1.fr (C. Deleuze-Masquefa).
† These authors contributed equally to this work.

0968-0896/$ - see front matter © 2008 Elsevier Ltd. All rights reserved.
doi:10.1016/j.bmc.2008.05.022

This study was related to the pharmacochemistry of nitrogen heterocycles. The aim of this paper was to synthesize and to develop three chemical series, analogues of imiquimod (Fig. 1): the imidazo[1,2-*a*]quinoxalines, the imidazo[1,5-*a*]quinoxalines, and the pyrazolo[1,5-*a*]quinoxalines, in order to evaluate their potential anti-cancer properties, in vitro against a variety of human cancer cell lines, and in vivo on melanoma by comparison with fotemustine (Fig. 1), one of the main drug used in clinic to treat human melanoma.

## 2. Results

### 2.1. Chemistry

#### 2.1.1. Library synthesis

For the preparation of the 1*H*-imidazo[1,5-*a*]quinoxaline derivatives, the procedure presented in Scheme 1 was used. In general, treatment of ortho-fluoronitrobenzene with imidazole and an excess of potassium carbonate formed compound **1** in 95% overall yield. After halogenation with *N*-bromosuccinimide, compounds **3a** and **3b** were obtained through Suzuki cross-coupling reactions with yields of 94% and 54%, respectively. Attempted reduction of the nitro group by hydrogenation resulted in the formation of **4a** and **4b** with yields of 45% and 94%, respectively. The formation of the tricyclic compounds **5a** and **5b** was obtained after addition of carbonyldiimidazole by intramolecular cyclization of **4a** and **4b**, respectively. The chlorination of **5a** and **5b** by phosphorus oxychloride and substitution by an adapted amine formed the **7a** and **7b** compounds with yields of 53% and 86%, respectively.

The synthesis of the 1*H*-pyrazolo[1,5-*a*]quinoxaline derivatives is illustrated in Scheme 2.

Dimer **8** resulted from the bimolecular condensation of the 3-isobutyl-1*H*-pyrazole-5-carboxylic acid, in presence of thionyl chloride in 80% overall yield. Product **8** was coupled with orthofluoroaniline to give the intermediate **9**, with a yield of 46%. The tricyclic compound **10** was obtained via an intramolecular cyclization of **9** in the presence of sodium hydride and dimethylacetamide as solvent with 80% yield. Treatment of compound **10** with phosphorus oxychloride yielded to 50% of compound **11** which was coupled with methylamine (series **a**) and dimethylamine (series **b**) to form **12a** and **12b** with average yields of 75% and 85%, respectively. The same strategy was applied to obtain the monosubstituted 1*H*-imi-

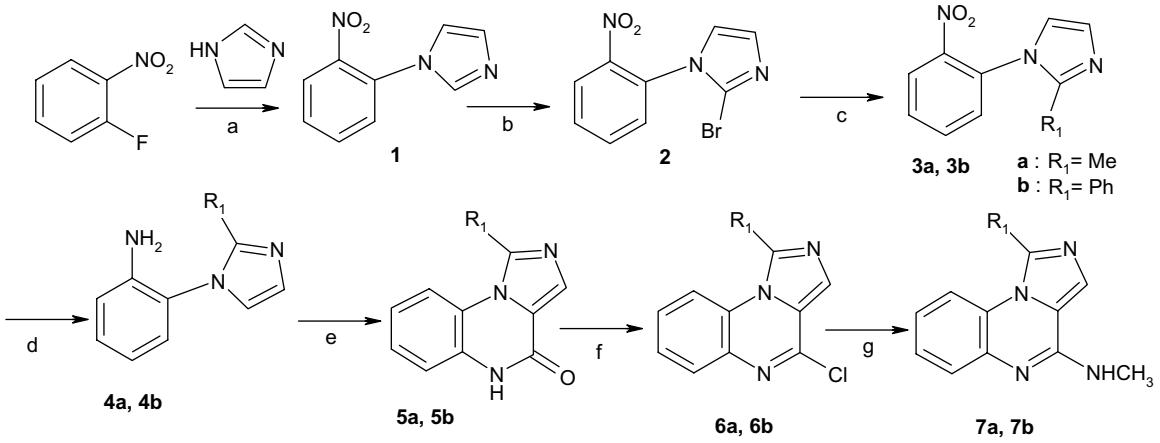


**Scheme 1.** Synthesis of *1H*-imidazo[1,5-*a*]quinoxaline derivatives. Reagents and conditions: (a) MeCN, reflux; (b) NBS, MeCN, reflux; (c) $R_1$-$B(OH)_2$, $Na_2CO_3$, DME, $Pd(PPh_3)$; (d) $H_2$/Pd-C, EtOH; (e) $Im_2CO$, $PhCl_2$, reflux; (f) $POCl_3$, reflux; (g) $R'NH_2$, EtOH.

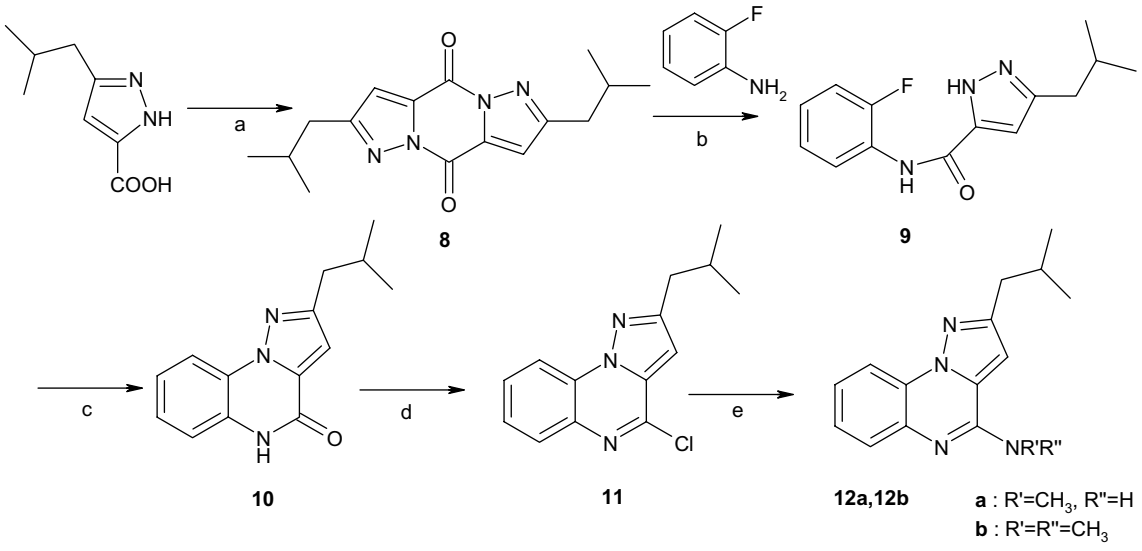


**Scheme 2.** Synthesis of *1H*-pyrazolo[1,5-*a*]quinoxaline derivatives. Reagents and conditions: (a) $SOCl_2$ reflux, 18 h; (b) NaHMDS, THF, 5 h; (c) NaH, DMA, reflux, 10 h; (d) $POCl_3$, reflux, 6 h; (e) EtOH, R′R″NH, 20 h, rt.

dazo[1,5-*a*]quinoxalines **17a** and **17b** starting from imidazole-4-carboxylic acid (Scheme 3).

All synthesized compounds with their corresponding p$K_a$ and log*P* calculated values are presented in Table 1. The 1*H*-imi-

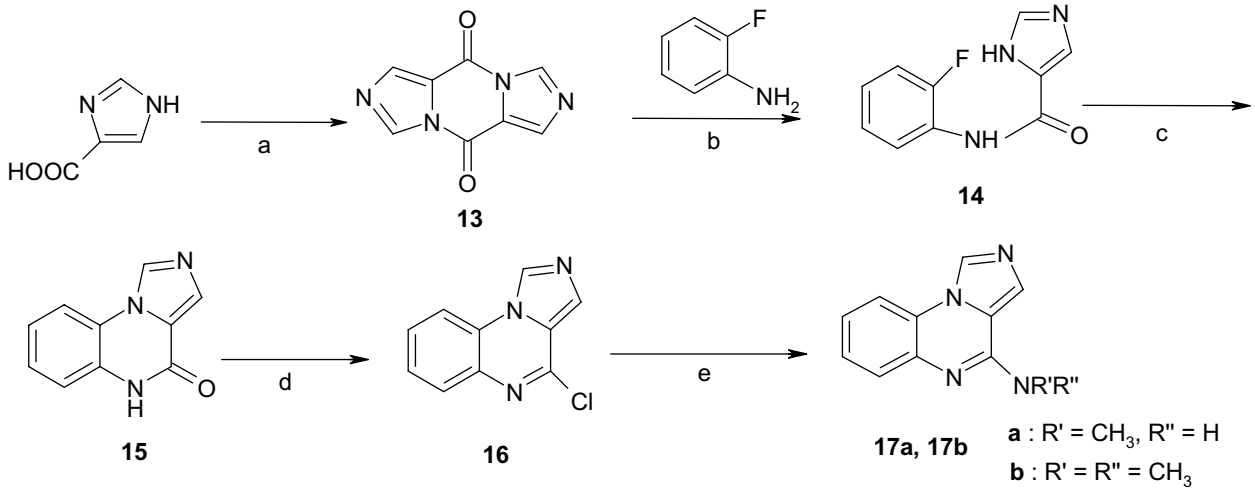


**Scheme 3.** New synthesis of the monosubstituted 1*H*-imidazo[1,5-*a*]quinoxaline derivatives. Reagents and conditions: (a) $SOCl_2$ reflux, 18 h; (b) NaHMDS, THF, 5 h; (c) NaH, DMA, reflux, 10 h; (d) $POCl_3$, reflux, 6 h; (e) EtOH, R′R″NH, 20 h, rt.

**Table 1**
1*H*-Imidazo[1,5-*a*]quinoxaline, 1*H*-imidazo[1,2-*a*]quinoxaline and 1*H*-pyrazolo[1,5-*a*]quinoxaline: formulas and in vitro cytotoxic activities against A375 human melanoma cell line

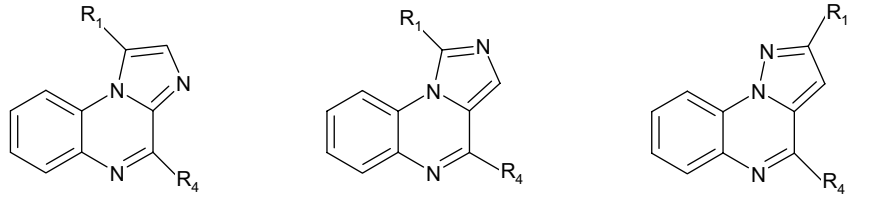

Imidazo[1,2-*a*]quinoxaline | Imidazo[1,5-*a*]quinoxaline | Pyrazolo[1,5-*a*]quinoxaline

| Compounds | $R_1$ | $R_4$ | Formula | $IC_{50}$ (μM)[a] against A375 cell line | p$K_a$* | Log*P** |
|---|---|---|---|---|---|---|
| *Imidazo[1,2-a]quinoxalines* | | | | | | |
| **EAPB0103** | $(CH_3)_2$–CH–$CH_2$– | $CH_3$–NH– | $C_{15}H_{18}N_4$ | 31.6 ± 2.0 | 5.61 ± 0.4 | 3.91 ± 1.42 |
| **EAPB0203** | $C_6H_5$–$(CH_2)_2$– | $CH_3$–NH– | $C_{19}H_{18}N_4$ | 1.57 ± 0.56 | 5.61 ± 0.4 | 4.91 ± 1.42 |
| **EAPB0202** | $C_6H_5$–$(CH_2)_2$– | $NH_2$– | $C_{18}H_{16}N_4$ | 2.35 ± 0.15 | 5.13 ± 0.4 | 4.97 ± 1.42 |
| **EAPB0201** | $C_6H_5$–$(CH_2)_2$– | Cl– | $C_{18}H_{14}ClN_3$ | 24.0 ± 0.5 | −1.57 ± 0.4 | 4.53 ± 1.27 |
| **EAPB0104** | $(CH_3)_2$–CH–$CH_2$– | $(CH_3)_2$–N– | $C_{16}H_{20}N_4$ | 66.3 ± 7.5 | 5.73 ± 0.4 | 3.33 ± 1.42 |
| **EAPB0204** | $C_6H_5$–$(CH_2)_2$– | $(CH_3)_2$–N– | $C_{20}H_{20}N_4$ | 80.1 ± 7.0 | 5.73 ± 0.4 | 4.32 ± 1.42 |
| **EAPB0206** | $C_6H_5$–$(CH_2)_2$– | $OCH_3$ | $C_{19}H_{17}N_3O$ | 47.8 ± 5.0 | 0.85 ± 0.4 | 4.56 ± 1.42 |
| **EAPB0105** | $(CH_3)_2$–CH–$CH_2$– | 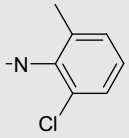 | $C_{21}H_{21}ClN_4$ | >400 | 2.25 ± 0.4 | 4.56 ± 1.42 |
| **EAPB0205** | $C_6H_5$–$(CH_2)_2$– | 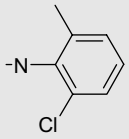 | $C_{25}H_{21}ClN_4$ | 329 ± 63 | 2.25 ± 0.4 | 7.25 ± 1.43 |
| *Imidazo[1,5-a]quinoxalines* | | | | | | |
| **17a** | H | $CH_3$–NH– | $C_{11}H_{10}N_4$ | 85.3 ± 7.0 | 6.50 ± 0.4 | 0.93 ± 1.07 |
| **17 b** | H | $(CH_3)_2$–N– | $C_{12}H_{12}N_4$ | 121 ± 17 | 6.62 ± 0.4 | 0.95 ± 1.08 |
| **7a** | $C_6H_5$– | $CH_3$–NH– | $C_{17}H_{14}N_4$ | >400 | 6.45 ± 0.4 | 3.38 ± 1.09 |
| **7b** | $CH_3$– | $CH_3$–NH– | $C_{12}H_{12}N_4$ | 100 ± 9 | 7.33 ± 0.4 | 1.19 ± 1.08 |
| *Pyrazolo[1,5-a]quinoxalines* | | | | | | |
| **12a** | $(CH_3)_2$–CH–$CH_2$– | $CH_3$–NH– | $C_{15}H_{18}N_4$ | 78.6 ± 7.8 | 6.20 ± 0.4 | 3.38 ± 1.06 |
| **12b** | $(CH_3)_2$–CH–$CH_2$– | $(CH_3)_2$–N– | $C_{16}H_{20}N_4$ | 101 ± 5 | 6.32 ± 0.4 | 3.40 ± 1.06 |
| **Imiquimod** | | | | 70.3 ± 4.3 | | |
| **Fotemustine** | | | | 173 ± 24 | | |

[a] $IC_{50}$, concentration of the compound (μM) producing 50% cell growth inhibition after 96 h of drug exposure, as determined by the MTT assay. Each experiment was run at least three times, and the results are presented as average values ± standard deviation.

* p$K_a$ and log*P* values are calculated using the ACDlabs software.

dazo[1,2-*a*]quinoxaline substituted derivatives were obtained as previously described.[15]

### 2.1.2. In vitro biological activity

All compounds were firstly evaluated for their cytotoxic activity in vitro against the A375 human melanoma cell line by comparison with imiquimod and fotemustine used as references. Concentrations of the compounds which produced 50% cell growth inhibition ($IC_{50}$ values) are summarized in Table 1 for the imidazo- and pyrazoloquinoxaline compounds, and for fotemustine and imiquimod. Among the compounds tested, **EAPB0203** ($IC_{50}$ = 1.57 μM) and **EAPB0202** ($IC_{50}$ = 2.35 μM) exhibited the highest cytotoxic activities. **EAPB0203** containing phenethyle as substituent at position 1 and methylamine at position 4 was the 'lead' compound with an activity against A375 cell line 110 times higher than fotemustine ($IC_{50}$ = 173 μM) and 45 times higher than imiquimod ($IC_{50}$ = 70 μM). The **EAPB0202** ($R_1$ = phenethyl and $R_4$ = amine) had an activity very close to that of **EAPB0203** (almost 2 times more active than **EAPB0202**) with an $IC_{50}$ value 70 times lower than fotemustine and 30 times lower than imiquimod. The **EAPB0103** compound having isobutyle at position 1 and methylamine at position 4 exhibited an interesting activity; this compound is 7 times more active than fotemustine and 3 times more active than imiquimod. The **EAPB0201** ($R_1$ = phenethyl and $R_4$ = chloro) also presents a good cytotoxic activity, this compound is 2 and 6 times more active than imiquimod and fotemustine, respectively. The other compounds, substituted or unsubstituted at position 1 and bearing dimethylamine or chloromethylaniline as substituent at position 4, are less potent and have $IC_{50}$ values between 20 and 300 μM. The cytotoxic activities of **7a** and **EAPB0105** have not been evaluated due to the very low solubility of these compounds in the culture medium. The pyrazolo[1,5-*a*]quinoxaline analogue **12a** showed similar activity than imiquimod.

Since **EAPB0203** exhibited the highest activity against the A375 melanoma cell line, we further evaluated its cytotoxic activity against the following human cell lines: M4Be and RPMI-7591 (melanoma), LS174T (colon cancer), MCF7 (breast cancer), and Raji (B lymphoma). The $IC_{50}$ values are illustrated in Table 2. The most interesting results were obtained on M4Be and RMPI-7591. **EAPB0203** exhibited cytotoxic activity 30-130 times higher than fotemustine, with $IC_{50}$ values of 2.58 and 4.23 μM, respectively. In addition **EAPB0203** showed a cytotoxic activity (3 times less potent) similar to irinotecan on LS174T cell line.

### 2.1.3. In vivo activity

The 50% lethal dose ($LD_{50}$) of **EAPB0203** was determined, in Swiss mice, after intraperitoneal administrations at doses ranging from 30 to 300 mg/kg. At the highest doses, **EAPB0203** appeared to be non toxic.

Previous studies have shown that **EAPB0203** is a potent in vitro growth inhibitor for human melanoma cell lines with a cytotoxic activity higher than fotemustine used as reference. To further evaluate the in vivo induction of melanoma death by **EAPB0203** we proceeded as described in materials and methods. Tumor size is the most common parameter used to assess effective anti-cancer treatment in preclinical models. The **EAPB0203** treatments were well tolerated without apparent side-effects or weight losses. As expected, M4Be xenografts grew progressively using the vehicle control. In contrast, in mice treated with **EAPB0203** or fotemustine, a highly significant delay in tumor growth was observed (Fig. 2). At highest doses (20 mg/kg), from day 18 to day 55, the simple contrast test showed a high significant difference in tumor growth between the **EAPB0203** and the control groups (*P* values ranging from 0.0026 to 0.00004). Lower significant differences were observed between the fotemustine and the control groups (not significant at days 18 through 24, 34, 37, and 55; and *P*: 0.014 to 0.0024 at days 27, 31, 41 through 51). Most interesting, **EAPB0203** treatment produced a statistically significant decrease in tumor growth at days 21, 24, 41, and 44 compared to the fotemustine treatment. Results are presented in Figure 2. At low doses (5 mg/kg), the variations in tumor growth according to the treatment group have the same profile than at high doses (data not shown) but lower significant differences were observed. Between fotemustine and **EAPB0203**, significant difference occurred on day 34.

Efficacy of treatment is dose-related. In mice receiving **EAPB0203**, the decrease in tumor growth was statistically higher on days 18 ($P = 0.026$), 21 ($P = 0.0058$), 24 ($P = 0.0073$), 31 ($P = 0.0033$), and 34 ($P = 0.016$) at the 20 mg/kg dose than at the 5 mg/kg dose. In animals treated by fotemustine, significant differences occurred at days 24 ($P = 0.017$), 27 ($P = 0.019$), 31 ($P = 0.0046$), and 34 ($P = 0.0052$).

In the control group, all mice were sacrificed on day 55. In the fotemustine group (20 mg/kg), all mice were killed on day 76, since tumor volumes were superior to 2 $cm^3$, while in the **EAPB0203** group (20 mg/kg), one mouse (1/6) was still alive with a tumor volume less than 2 $cm^3$ (the limit fixed by the protocol).

## 3. Discussion

Imiquimod is a low-molecular-weight immune response modifier that can induce the synthesis of interferon-α and other cytokines in a variety of cell types. Imiquimod has potent anti-viral and anti-tumor properties. Several mechanisms by which this compound exerts its activity have been mentioned. Many studies[11,16,17] show that imiquimod activates immune cells via the Toll-like receptor 7 (TLR7)-MyD88-dependent signalling pathways. Based on some reports[14,18] of apoptosis in skin cancer, imiquimod exerts a direct pro-apoptotic effect against human melanoma. It is able to induce apoptosis in malignant melanoma cells both in vitro and in vivo in a rather tumor-selective manner. Imiquimod-induced apoptosis in tumor cells could not be antagonized by functional blockage of various membrane-bound death receptors,

**Table 2**
$IC_{50}$ values for imiquimod, fotemustine, methotrexate, irinotecan, doxorubicin, and **EAPB0203** against A375, M4Be, and RMPI-7591 (melanoma cell lines), LS174T (colon cancer), MCF7 (breast cancer), and Raji (B lymphoma) human cell lines

| Compounds | $IC_{50}$ (μM)[a] | | | | | |
|---|---|---|---|---|---|---|
| | A375 | M4Be | RPMI-7591 | MCF7 | LS174T | Raji |
| Fotemustine | 173 ± 24 | 326 ± 34 | 125 ± 49 | | | |
| Doxorubicin | | | | 0.13 ± 0.01 | | |
| Irinotecan | | | | | 1.16 ± 0.07 | |
| Methotrexate | | | | | | 0.04 ± 0.005 |
| Imiquimod | 70.3 ± 4.3 | 33.5 ± 7.7 | 53.7 ± 9.8 | 145 ± 7 | 34.4 ± 9.7 | 139 ± 12 |
| **EAPB0203** | 1.57 ± 0.56 | 2.58 ± 0.40 | 4.23 ± 0.48 | 1.08 ± 0.46 | 4.12 ± 0.67 | 6.23 ± 0.06 |

[a] $IC_{50}$, concentration of the compounds (μM) producing 50% cell growth inhibition after 96 h of drug exposure, as determined by the MTT assay. Each experiment was run at least three times, and the results are presented as average values ± standard deviation.

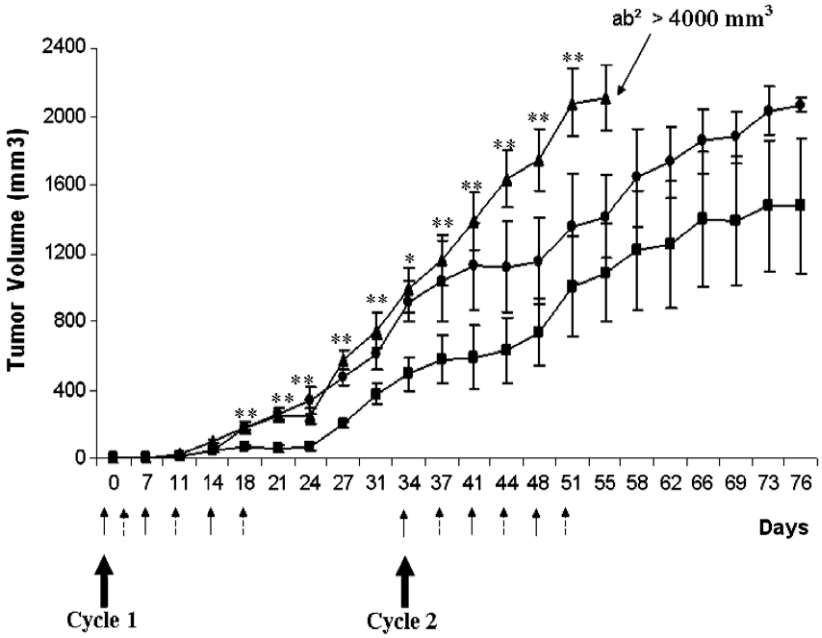


**Figure 2.** Effects of fotemustine (20 mg/kg once a week for 3 weeks) and **EAPB0203** (20 mg/kg twice a week for 3 weeks) on tumor growth ($ab^2$) in xenografted nude mice by M4Be melanoma cell lines. ↑, fotemustine and **EAPB0203** administrations; ⋮, **EAPB0203** administrations ▲, control mice; ■, **EAPB0203**; ●, fotemustine. Data are the mean of one experiment carried out on six mice. Error bars represent SEM. Significant difference between the 3 treatment groups: *, $P < 0.05$; **, $0.002 < P < 0.009$; ***, $P \leqslant 0.001$.

including Fas/APO-1 (CD95), TRAIL, and TNF receptors, which suggests that imiquimod-inducing apoptosis is independent from apoptosis mediated by membrane-bound death receptors. Its tumor-selective pro-apoptotic activity is correlated with translocation of cytochrome c from the mitochondria to the cytosol by shifting the mitochondria-associated Bcl-2/Bax ratio, and activating caspases 9 and 3. Imidazo[1,2-*a*]quinoxalines are imiquimod analogues that inhibit cyclic nucleotide phosphodiesterase enzymes 4.[15] Furthermore, in studies on murine fibroblast L929 cells, we recently showed that these imidazo[1,2-*a*]quinoxalines activate the p38 MAPK pathway, and inhibit the PI3K pathway.[19] Furthermore, we recently demonstrated that one of these compounds (**EAPB0203**) induced inhibition of cell proliferation, G2/M cell cycle arrest, and apoptosis in HTLV-I transformed and HTLV-I-negative malignant T cells as well in fresh adult T-cell leukaemia (ATL) cells, while normal resting or activated T lymphocytes were resistant. **EAPB0203** initiated the apoptotic process via the intrinsic cell death pathway converging at the mitochondria.[21]

In the present study, we report the synthesis and preliminary pharmacological evaluation of a new series of imiquimod's analogues, the imidazo/pyrazoloquinoxaline derivatives. Imidazoquinoxalines were prepared via two different methods, the first one previously described[15] and the second one is presented in Scheme 1. The first method[15] was used to synthesize the imidazo[1,2-*a*]quinoxaline compounds which were obtained in seven steps in good yields. The second method outlined in Scheme 1 was employed for the synthesis of the imidazo[1,5-*a*]quinoxaline compounds. Using these two methods, a limited number of analogues were obtained. Actually, the alkyl or aryl substitution at the $R_1$ position must be done at the beginning steps of the synthesis leading to a low variability in the moieties on the imidazole cycle. Likewise, the purifications after each step caused further limitations of the synthetic process. Our framework was to optimize the methods of synthesis (i) to obtain a common strategy for the three chemical series, (ii) to reduce the number of purification steps, and (iii) to increase the structural diversity of these series essential for the SAR studies. The procedure presented in Scheme 2 was used to prepare the pyrazolo[1,5-*a*]quinoxaline derivatives.[20] This method not only reduced the number of purification steps but also led us to propose a new common and efficient route for the preparation of the unsubstituted imidazo[1,5-*a*]quinoxalines on the imidazole core (Table 1) starting from the unsubstituted carboxylic acid (Scheme 3). This new strategy also permitted the introduction the $R_1$ substituent at the last steps of the procedure with different commercial Suzuki cross coupling reagents (syntheses under study, data not shown).

All compounds were screened in vitro against the human melanoma cell line A375. First, we assessed the influence of the substituent at the $R_4$ position by the introduction of four types of amines with increasing steric hindrance **EAPB0202**, **EAPB0203**, **EAPB0204**, and **EAPB0205** (Table 1). At $R_4$ position, the methylamino group (**EAPB0203**) appears to be essential for the potency. Indeed, accessibility at the electronic doublet of the nitrogen on this position of the heterocycle might be critical for activity, thanks to the low steric bulk of this secondary amine. No significant differences were observed between the p$K_a$ and log*P* calculated values (Table 1) of this series of compounds which are all substituted by an amino group at the $R_4$ position. We next focused our attention on the substitution on the imidazole core with the objective to improve in vitro potency against A375 cells. We also explored the effect of the incorporation of a phenethyle substituent at the $R_1$ position. **EAPB0203**, bearing phenethyle on $R_1$, significantly enhanced the activity ($IC_{50}$ = 1.57 μM) by creation of an Π interaction necessary for its binding. The improved bioactivity of the **EAPB0203** compound may be attributed to the additional effect and the synergy between the methylamino and phenethyle groups in addition to the basic pharmacophore that might be defined by the sequence of the three intracyclic nitrogens of the imidazo[1,2-*a*]quinoxaline series. Overall, the other analogues appeared to be less potent. In a general way, it is noticed that the imidazo[1,2-*a*]quinoxaline derivatives have a better activity than the two other series of compounds, but this still remains to be proven by comparison with a larger variety of imidazo-/pyrazolo[1,5-*a*]quinoxaline derivatives.

Two drugs are approved in the European Union for treatment of advanced or metastatic melanoma: dacarbazine and fotemustine.[22]

Furthermore, imiquimod was recently approved for treatment of different cutaneous cancers.

**EAPB0203** displayed potent cellular cytotoxic activity with micromolar $IC_{50}$ values against different human cancer cell lines and was compared to fotemustine and imiquimod (Table 2). Upon such encouraging results, **EAPB0203** was selected for detailed in vivo studies. In human melanoma (M4Be) xenografted athymic mice, **EAPB0203**, administered twice a week at 20 mg/kg, has approached a significant delay in tumor growth and also a decrease in tumor size compared to that of control and fotemustine groups (Fig. 2). Interestingly, a stabilization and even an arrest in tumor growth were observed after each treatment cycle. The efficacy of treatment is dose-related. The **EAPB0203** treatment was well tolerated without side-effects.

## 4. Conclusion

In this paper, we have reported the synthesis of imidazoquinoxaline and pyrazoloquinoxaline derivatives, and their in vitro cytotoxic activity against human melanoma cell lines and the in vivo anti-proliferative activity of the **EAPB0203** derivative on melanoma. The synthesis was based on a bimolecular condensation of a carboxylic acid, followed by a coupling with orthofluoroaniline, an intramolecular cyclisation and a substitution with appropriate amines. This strategy will be the starting point for the development of other compounds. The incorporation of phenethyle as moiety at the $R_1$ position and methylamine at the $R_4$ position led to the **EAPB0203** compound with enhanced cytotoxic activity against A375 human melanoma cell line. Its $IC_{50}$ (1.57 μM) was 110 times lower than fotemustine ($IC_{50}$ = 173 μM), and **EAPB0203** was 45 times more potent than imiquimod ($IC_{50}$ = 70 μM). Interestingly, compared to imiquimod and fotemustine, this compound also had lower $IC_{50}$ values (30–130-fold) against the two other melanoma cell lines tested. In vivo, **EAPB0203** had potent anti-tumor activity on human melanoma (M4Be) xenografted nude mice. Our results support a potential therapeutic role of **EAPB0203** in the treatment of malignant melanoma and prompt us to modulate the chemical structure of this lead molecule to optimize its effect. Further studies are now in progress to study the mode of action and should lead to an interesting class of new anti-cancer drugs with innovating mechanism of action.

## 5. Experimental

### 5.1. Chemistry

All solvents and reagents were obtained from commercial sources and used without further purification unless indicated otherwise. $^1H$ and $^{13}C$ NMR spectra were recorded using a Bruker AC 300 spectrometer. Chemical shifts are reported in parts per million (ppm) from the tetramethylsilane resonance in the indicated solvent. Coupling constants are reported in Hertz (Hz), spectral splitting partners are designed as follow: singlet (s); doublet (d); triplet (t); multiplet (m). Column chromatography was performed on Merck silica gel 60 (200–400 mesh). Elemental analysis was carried out at the Microanalytical Central Department (Montpellier, France). All melting points are determined using köfler hot plate melting point apparatus and are not corrected. $pK_a$ and log*P* values are calculated using the ACDLabs software (Toronto, Canada).

#### 5.1.1. 2-Chloro-1-isobutyl-6-methylphenyl-*N*-methylimidazo [1,2-*a*]quinoxalin-4-amine (EAPB0105)

To a solution of 6-chloro-3-methylaniline (89 mg, 0.63 mmol) in THF (12 ml), was added a solution of sodium bis(trimethylsilyl)amide (4 mL, 4 mmol, 1.0 M in THF), and the reaction mixture was heated to reflux for 0.5 h. The reaction mixture was cooled to room temperature and the 4-chloro-1-isobutylimidazo[1,2-*a*]quinoxaline[15] (150 mg, 0.5 mmol) in THF (10 mL) was added. The mixture was again heated to reflux for 0.5 h and then cooled to room temperature and stopped with acetic acid until pH 7. The reaction mixture was concentrated in vacuum followed by addition of water and saturated sodium bicarbonate. The solid was collected by filtration, washed with water and hexane, and dried under high vacuum to give **EAPB0105** (110 mg, 60%); $^1H$ NMR (300 MHz, $CDCl_3$-$d_6$): $\delta$ 8.01 (t, 1H), 7.6 (m, 3H), 7.5 (d, 1H), 7.38 (d, 1H), 7.06 (s, 1H), 6.67 (t, 1H), 3.00 (t, 2H), 2.2 (m, 5H), 0.81 (t, 6H). $^{13}C$ NMR (300 MHz, $CDCl_3$): $\delta$ 142.61, 140.68, 139.55, 131.44, 130.32, 129.71, 129.19, 128.07, 126.78, 126.27, 125.55, 123.44, 122.79, 114.36, 33.68, 32.75, 21.99, 18.10. Anal. calcd for $C_{21}H_{21}ClN_4$: C, 69.13; H, 5.80; N, 15.35. Found: C, 69.33; H, 5.42; N, 15.65.

#### 5.1.2. 2-Chloro-6-methylphenyl-*N*-methyl-1-phenethylimidazo [1,2-*a*]quinoxalin-4-amine (EAPB0205)

**EAPB0205** was prepared with the same procedure as the one for the preparation of EAPB0105; using 4-chloro-1-phenethylimidazo[1,2-*a*]quinoxaline[15] (200 mg, 0.65 mmol) in 10 ml of THF. **EAPB0205** was obtained as a white solid (120 mg, 45%); $^1H$ NMR (300 MHz, $CDCl_3$-$d_6$): $\delta$ 7.93 (d, 1H), 7.49 (d, 1H), 7,56 (m, 3H), 7.39 (d, 1H), 7.24 (m, 5H), 6.73 (t, 1H), 3.3 (t, 4H), 2.23 (s, 1H). $^{13}C$ NMR (300 MHz, $CDCl_3$): $\delta$ 143.12, 142.57, 140.69, 139.77, 137.67, 131.44, 130.42, 130.12, 129.71, 129.19, 128.81, 126.78, 126.44, 126.27, 125.55, 124.38, 124.3, 114.22, 35.17, 23.83, 18.10. Anal. calcd for $C_{25}H_{21}ClN_4$: C, 72.72; H, 5.13; N, 13.57. Found: C, 72.41; H, 5.38; N, 13.39.

#### 5.1.3. 1-(2-Nitrophenyl)-1*H*-imidazole (1)

A mixture of 2-nitrofluorobenzene (14.85 mL, 0.142 mol), imidazole (14.9 g, 0.128 mol), and 40 g of $K_2CO_3$ in 200 ml of $CH_3CN$ was heated to reflux for 24 h. The solvent was removed under vacuum, and the residue was slurred in 200 mL of $CH_2CL_2$, washed twice with 200 mL of water, dried over $Mg_2SO_4$, and the solvent was removed under vacuum. We obtained 95% of **1** as a yellow solid. $^1H$ NMR (300 MHz, $CDCl_3$): $\delta$ 9.12 (s, 1H), 7.58 (d, 1H), 7.42 (d, 1H), 7.37 (d, 1H), 7.26 (d, 1H), 7.10 (m, 3H, ArH). Anal. calcd for $C_9H_7N_3O$: C, 57.14; H, 3.70; N, 22.22. Found: C, 56.99; H, 3.9; N, 22.06.

#### 5.1.4. 2-Bromo-1-(2-nitrophenyl)-1*H*-imidazole (2)

To a solution of **1** (5 g, 0.27 mmol) in dry acetonitrile (250 mL), *N*-bromosuccinimide (5.65 g, 0.032 mmol) was added. The reaction mixture was stirred to reflux for 3 h. The solvent was removed under vacuum and the residue was slurred in 250 mL of $CH_2CL_2$, washed twice with a solution of 5% $NaHCO_3$, dried over $MgSO_4$, and purified by column chromatography ($CH_2Cl_2$-MeOH, 98:2, v/v) to give 50% of **2**. $^1H$ NMR (300 MHz, $CDCl_3$): $\delta$ 8.03 (d, 1H), 7.70 (d, 1H), 7.47 (t, 1H), 7.33 (d, 1H), 7.09 (m, 2H). Anal. calcd for $C_9H_6N_3O_2Br$: C, 40.30; H, 2.24; N, 15.42. Found: C, 40.65; H, 2.01; N, 15.52.

#### 5.1.5. 2-Methyl-1-(2-nitrophenyl)-1*H*-imidazole (3a)

To a mixture of **2** (2 g, 7.46 mmol) and $Pd(PPh_3)_4$ (0.8 g, 0.7 mmol) in 1,4-dioxane (34 mL), 1.4 mL of the trimethylboroxine was added followed by $Na_2CO_3$ (2.37 g, 22.38 mmol) in 5 mL of water. The reaction mixture was heated to 75 °C with vigorous stirring under nitrogen atmosphere. After 24 h, a second portion of trimethylboroxine was added. After that, the mixture was poured into water and extracted with dichloromethane. The combined organic extracts were washed with water, dried over calcium chloride, and concentrated to dryness under vacuum. The crude products were purified by column chromatography (silica gel, elu-

tion with $CH_2Cl_2$–MeOH, 97:7, v/v) to give **3a** (yield, 94%). $^1$H NMR (300 MHz, $CDCl_3$): $\delta$ 7.40 (m, 2H), 7.22 (d, 1H), 7.11 (d, 1H), 7.01 (m, 2H), 2.3 (s, 3H). Anal. calcd for $C_{10}H_9N_3O_2$: C, 59.11; H, 4.43; N, 20.69. Found: C, 59.32; H, 4.65; N, 20.51.

#### 5.1.6. 1-(2-Nitrophenyl)-2-phenyl-1*H*-imidazole (3b)

**3b** was prepared from **2** following the protocol described for **3a** (i.e., from **2** (2 g, 7.46 mmol), $Pd(PPh_3)_4$ (0.5 g, 0.4 mmol) in DME (85 mL), 2 × 1 g (16.4 mmol) of phenylboronic acid and $Na_2CO_3$ (2.37 g, 22.38 mmol) in 5 mL of water). The crude products were purified by column chromatography (silica gel, elution with $CH_2Cl_2$–MeOH, 97:7, v/v) to give **3b** (yield, 88%). $^1$H NMR (300 MHz, $CDCl_3$): $\delta$ 8.45 (dd, 2H), 7.60 (t, 1H), 7.57 (m, 2H), 7.40 (m, 5H), 7.02 (d, 1H). Anal. calcd for $C_{15}H_{11}N_3O_2$: C, 67.92; H, 4.15; N, 15.85. Found: C, 67.75; H, 4.47; N, 15.70.

#### 5.1.7. 2-(2-Methylimidazol-1-yl)phenylamine (4a)

Compound **3a** (0.3 g, 1.48 mmol) was dissolved in 20 mL of ethanol with 0.3 g of 10% palladium on carbon and hydrogenated for 2 h. The catalyst was removed by filtration, and the residue concentrated under vacuum and purified by column chromatography on silica gel using $CH_2Cl_2$–MeOH (97:3) as eluent to yield 43% of **4a**. $^1$H NMR (300 MHz, DMSO-$d_6$): $\delta$ 7.36 (m, 2H), 7.03 (d, 1H), 6.90 (m, 2H), 6.79 (d, 1H), 2.1 (s, 3H). Anal. calcd for $C_{10}H_{11}N_3$: C, 69.36; H, 6.36; N, 24.28. Found: C, 69.5; H, 6.11; N, 24.12.

#### 5.1.8. 2-(2-Phenylimidazol-1-yl)phenylamine (4b)

This compound was prepared as described for **4a** to obtain **4b** (yield, 93%) (i.e., from **3b** (1.31 g, 5 mmol), EtOH (60 mL), and 0.3 g of 10% palladium on carbon). $^1$H NMR (300 MHz, DMSO-$d_6$): $\delta$ 7.36 (m, 2H), 7.25 (m, 5H), 7.12 (t, 1H), 6.8 (m, 2H), 3.67 (s, 2H, $-NH_2$). Anal. calcd for $C_{15}H_{13}N_3$: C, 76.59; H, 5.53; N, 17.97. Found: C, 76.72; H, 5.34; N, 18.02.

#### 5.1.9. 1-Methyl-5*H*-imidazo[1,5-*a*]quinoxalin-4-one (5a)

Compound **4a** (1.38 g, 8 mmol) and carbonyldiimidazole (1.55 g, 9.57 mmol) were dissolved in 83 mL of 1,2-dichlorobenzene and heated to reflux under $N_2$ for 2 h. After cooling to room temperature, the residue was slurred with $CH_2Cl_2$, washed with water, and dried over $MgSO_4$. The product was purified by chromatography on silica gel using $CH_2Cl_2$–MeOH (97:3, v/v) as eluent to give 62% of **5a**. $^1$H NMR (300 MHz, DMSO-$d_6$): $\delta$ 8.1 (d, 1H), 7.7 (s, 1H), 7.37 (m, 2H), 7.25 (t, 1H), 2.5 (s, 3H). Anal. calcd for $C_{11}H_9N_3O$: C, 68.38; H, 4.66; N, 16.09. Found: C, 68.49; H, 4.41; N, 16.20.

#### 5.1.10. 1-Phenyl-5*H*-imidazo[1,5-*a*]quinoxalin-4-one (5b)

This compound was prepared as described for **5a**, that is, from **4b** (1.08 g, 4.6 mmol) and carbonyldiimidazole (0.9 g, 5.51 mmol) in 56 mL of 1,2-dichlorobenzene. After cooling to room temperature, the solid was filtered and washed with diethylether to give **5b** (yield, 42%). $^1$H NMR (300 MHz, DMSO-$d_6$): $\delta$ 7.9 (s, 1H), 7.72 (m, 5H), 7.35 (m, 2H), 7.01 (d, 1H), 6.9 (t, 1H). Anal. calcd for $C_{16}H_{11}N_3O$: C, 73.31; H, 4.21; N, 16.09. Found: C, 73.42; H, 4.32; N, 16.21.

#### 5.1.11. 4-Chloro-1-methylimidazo[1,5-*a*]quinoxaline (6a)

A mixture of **5a** (0.9 g, 4.5 mmol) and 10 mL of phosphorus oxychloride was heated at reflux under $N_2$ for 5 h. The excess of $POCl_3$ was removed under vacuum, and the residue dissolved in 20 ml $CH_2Cl_2$, washed with 5% $Na_2CO_3$, dried over $MgSO_4$, and purified by chromatography on silica gel using $CH_2Cl_2$–MeOH (95:5, v/v). Concentration of the pure fractions provided 30% of **6a**. $^1$H NMR (300 MHz, $CDCl_3$): $\delta$ 8.29 (dd, 1H), 7.82 (dd, 1H), 7.7 (s, 1H), 7.54 (m, 2H), 3.04 (s, 3H). Anal. calcd for $C_{11}H_8N_3Cl$: C, 60.69; H, 3.68; N, 19.31. Found: C, 60.78; H, 3.92; N, 19.06.

#### 5.1.12. 4-Chloro-1-phenylimidazo[1,5-*a*]quinoxaline (6b)

**6b** was prepared from **5b** following the protocol described for **6a** (i.e., from **5b** (0.57 g, 2.18 mmol) and $POCl_3$ (5 mL)). A yellow solid was obtained after column chromatography purification as specified for **6a** (yield, 61%). $^1$H NMR (300 MHz, $CDCl_3$): $\delta$ 8.1 (s, 1H), 7.9 (dd, 1H), 7.5 (m, 5H), 7.4 (m, 2H), 7.32 (t, 1H). Anal. calcd for $C_{16}H_{10}N_3Cl$: C, 68.69; H, 3.58; N, 15.03. Found: C, 68.51; H, 3.39; N, 15.38.

#### 5.1.13. *N*-Methyl-1-methylimidazo[1,5-*a*]quinoxalin-4-amine (7a)

Methylamine (0.5 mL of a 40% (w/v) aqueous solution, 4 mmol) was added dropwise to a stirred solution of **6a** (0.3 g, 1.33 mmol) in absolute EtOH (7 mL) at room temperature. After 40 h, another portion of methylamine (0.5 mL of a 40% (w/v) aqueous solution, 4 mmol) was added and stirring was maintained for additional 3 h. The solvent was removed under reduced pressure and the residue was dissolved in $CH_2Cl_2$ (10 mL). The organic fraction was successively washed with 5% $NaHCO_3$ (15 mL) and water (15 mL), dried ($Na_2SO_4$), and concentrated under reduced pressure. The product was purified by column chromatography on silica gel eluting with $CH_2Cl_2$–MeOH (98:2, v/v) to yield a solid cream of **7a** (yield, 53%). $^1$H NMR (300 MHz, $CDCl_3$): $\delta$ 8.01 (d, 1H), 7.7 (d, 1H), 7.5 (s, 1H), 7.3 (t, 1H), 7.21 (t, 1H), 3.22 (d, 3H), 2.95 (s, 3H). $^{13}$C NMR (300 MHz, $CDCl_3$): $\delta$ 149.30, 142.34, 126.96, 126.33, 124.9, 122.85, 120.85, 119.78, 115.20, 30.84, 27.69. Anal. calcd for $C_{12}H_{12}N_4$: C, 67.92; H, 5.66; N, 26.41. Found: C, 67.52; H, 5.95; N, 26.36.

#### 5.1.14. *N*-Methyl-1-phenylimidazo[1,5-*a*]quinoxalin-4-amine (7b)

**7b** was prepared from **6b** following the protocol described for **7a**, that is, from **6b** (0.4 g, 1.4 mmol) and methylamine (0.12 g of 40% (w/v), 4 mmol). A yellow solid was obtained after column chromatography purification as specified for **7a** (yield, 86%). $^1$H NMR (300 MHz, $CDCl_3$): $\delta$ 7.6 (m, 4H), 7.56 (m, 3H), 7.2 (m, 2H), 6.93 (t, 1H), 3.22 (d, 3H). $^{13}$C NMR (300 MHz, $CDCl_3$): $\delta$ 149.31, 144.42, 138.31, 132.53, 129.76, 129.71, 129.00, 128.77, 126.96, 126.55, 124.11, 122.37, 122.31, 120.07, 116.25, 27.73. Anal. calcd for $C_{17}H_{14}N_4$: C, 74.45; H, 5.11; N, 20.40. Found: C, 74.10; H, 5.22; N, 20.57.

#### 5.1.15. 5,5-Diisobutyldipyrazolo[1,5-*a*]piperazine-5,10-dione (8)

The 3-isobutyl-1*H*-pyrazole-5-carboxylic acid (0.9 g, 5.35 mmol) in suspension in thionyl chloride (7 mL) was heated to reflux, under agitation for 18 h. The reaction mixture was cooled, then filtered and washed with toluene, and dried under high vacuum to obtain a white solid (yield, 80 %). $^1$H NMR (300 MHz, DMSO-$d_6$): $\delta$ 0.9 (d, 12H), 1.9 (m, 1H), 2.5 (d, 2H), 7.4 (s, 2H). Anal. calcd for $C_{16}H_{20}N_4O_2$: C, 64.00; H, 6.67; N, 18.67. Found: C, 64.31; H, 6.33; N, 18.56.

#### 5.1.16. 2-Fluoroaniline-3-isobutyl-1*H*-pyrazole-5-carboxamide (9)

To 2-fluoroaniline (0.734 mL, 7.6 mmol) in THF (8 mL), cooled in a −10 °C bath, 18.3 mL (18.30 mmol, 1.0 M) sodium bis-(trimethylsilyl)amide in THF was added. The mixture was stirred for 1 h, and a suspension of **8** (1.14 g, 3.8 mmol) in THF (15 mL) was added and let warm to room temperature. The mixture was stirred for 2 h, and acetic acid was added to pH 7. The reaction mixture was concentrated in vacuum followed by the addition of water and saturated $NaHCO_3$. The solid was collected by filtration, washed with water and cyclohexane, and dried under high vacuum to give **9** as a beige solid (yield, 46%).$^1$H NMR (300 MHz, DMSO-$d_6$): $\delta$ 7.85 (m, 1H), 7.25 (m, 1H), 7.15 (m, 2H), 6.5 (s, 1H), 2.46 (d, 2H), 1.88

(m, 1H), 0.85 (d, 6H). $^{19}$F NMR: 126. Anal. calcd for $C_{14}H_{16}N_3OF$: C, 64,37; H, 6.13; N, 16.09. Found: C, 64.09; H, 6.01; N, 16.25.

#### 5.1.17. 3-Isobutylpyrazolo[1,5-*a*]quinoxaline-pyrazine-6-(5*H*)-one (10)

A mixture of **9** (0.88 g, 3.37 mmol) and sodium hydrure (0.97 g, 4.04 mmol) in dimethylacetamide (25 mL) was heated to reflux for 6 h. The reaction mixture was then concentrated in vacuum followed by the addition of water and saturated ammonium chloride. The solid was collected by filtration, washed with water, and dried to give **10** (yield, 80%). $^1$H NMR (300 MHz, DMSO-$d_6$): $\delta$ 0.9 (d, 6H), 2 (m, 1H), 3.3 (s, 2H), 6.9 (s,1H), 7.3 (m, 4H), 8.05 (s, 1H). Anal. calcd for $C_{14}H_{15}N_3O$: C, 69.71; H, 6.22; N, 17.43. Found: C, 69.98; H, 6.51; N, 17.38.

#### 5.1.18. 6-Chloro-3-isobutylpyrazolo[1,5-*a*]quinoxaline (11)

To **10** (1.04 g, 4.3 mmol), 12 mL of phosphorus oxychloride was added and the mixture was heated to reflux for 6 h. The reaction mixture was concentrated under vacuum, and the residue was cooled in an ice bath. Water was added to the residue and neutralized with saturated $NaHCO_3$. The solid was collected by filtration and purified using column chromatography on silica gel to yield **11** as a yellow solid (yield, 50%). $^1$H NMR (300 MHz, DMSO-$d_6$): $\delta$ 0.9 (d, 6H), 2 (m, 1H), 3.3 (s, 2H), 6.9 (s,1H), 7.3 (m, 4H), 8.05 (s, 1H). Anal. calcd for $C_{14}H_{14}N_3OCl$: C, 64.74; H, 5.39; N, 16.18. Found: C, 64.52; H, 5.24; N, 16.33.

#### 5.1.19. 3-Isobutyl-*N*-methylpyrazolo[1,5-*a*]quinoxalin-4-amine (12a)

Methylamine (0.15 mL of a 40% (w/v) aqueous solution, 1.74 mmol) was added dropwise to a stirred solution of **11** (0.15 g, 0.57 mmol) in absolute EtOH (10 mL) at room temperature. After 40 h, another portion of methylamine (0.25 mL of a 40% (w/v) aqueous solution, 2.7 mmol) was added and stirring was maintained for additional 3 h. The solvent was removed under reduced pressure, and the residue was dissolved in $CH_2Cl_2$ (10 mL). The organic fraction was successively washed with 5% $NaHCO_3$ (15 mL) and water (15 mL), dried ($Na_2SO_4$), and concentrated under reduced pressure. The product was purified by column chromatography on silica gel with $C_6H_{12}$–EtOAc (70:30, v/v) as eluent to yield a cream solid (yield, 75%). Mp 145–150°C. $^1$H NMR (300 MHz, DMSO-$d_6$): $\delta$ 8.25 (dd, $J_1$ = *1.37 Hz*, $J_2$ = *7.8*, 1H), 7.7 (dd, $J_1$ = *1.46*, $J_2$ = *8.11*,1H), 7.3 (m, 2H), 6.37 (s, 1H), 4.95 (s, 1H), 3.25 (d, 3H), 3.75 (d, 2H), 2.08 (m, 1H), 0.95 (d, 6H).$^{13}$C NMR (300 MHz, DMSO-$d_6$): $\delta$ 152.43, 150.30, 139.7, 125.4, 125.16, 124.6, 123.7, 122.21, 112.21, 108.25, 35.10, 29.61, 28.57, 23.14. Anal. calcd for $C_{15}H_{18}N_4$: C, 70.84; H, 7.13; N, 22.03. Found: C, 70.37; H, 7.44; N, 21.99.

#### 5.1.20. 3-Isobutyl-*N*,*N*-dimethylpyrazolo[1,5-*a*]quinoxalin-4-amine (12b)

**12b** was prepared from **11** following the protocol described for **12a**, that is, from dimethylamine (0.22 mL of a 40% (w/v) aqueous solution, 1.73 mmol) and **11** (0.15 g, 0.57 mmol) in absolute EtOH (10 mL). The product was purified by column chromatography on silica gel with $C_6H_{12}$–EtOAc (70:30, v/v) as eluent to give a white solid (yield, 83%). Mp 160–165°C. $^1$H NMR (300 MHz, DMSO-$d_6$): $\delta$ 8.25 (dd, $J_1$ = *1.32*, $J_2$ = *7.9*, 1H), 7.65 (dd, $J_1$ = *1.24*, $J_2$ = *9.12*, 1H), 7.3 (m, 2H), 6.6 (s, 1H), 3.3 (s, 6H), 2.75 (d, 2H), 2.09 (m, 1H), 1 (d, 6H). $^{13}$C NMR (300 MHz, DMSO-$d_6$): $\delta$ 149.79, 145.9, 140.85, 125.56, 125.42, 124.98, 124.00, 122.63, 114.26, 112.60, 39.48, 35.10, 29.61, 23.01. Anal. calcd: for $C_{16}H_{20}N_4$: C, 71.61; H, 7.51; N, 20.88. Found: C, 71.37; H, 7.62; N, 21.09.

#### 5.1.21. Diimidazo[1,5-*a*]piperazine-5,10-dione (13)

**13** was prepared from the imidazole-4-carboxylic acid (5 g, 44.6 mmol) and thionyl chloride (75 mL) following the protocol described for **8**. We obtained 4.7 g of a white solid (yield, 90–95%).$^1$H NMR (300 MHz, DMSO-$d_6$): $\delta$ 8.85 (s, 2H); 8.2 (s, 2H). Anal. calcd for $C_8H_4N_4O_2$: C, 51.33; H, 2.13; N, 29.79. Found: C, 51.23; H, 2.01; N, 29.56.

#### 5.1.22. (2-Fluoroaniline)-1*H*-imidazole-4-carboxamide (14)

**14** was prepared from **13** following the protocol described for **9**, that is, from 2-fluoroaniline (5.9 g, 53 mmol) in THF (26 ml), sodium bis-(trimethylsilyl)amide (133.0 mmol, 1.0 M in THF) and **13** (4.7 g, 24.0 mmol) in THF (30 mL). We obtained 7.50 g of **14** as a light beige solid (yield, 42%). $^1$H NMR (300 MHz, DMSO-$d_6$): $\delta$ 9.45 (s, 2H), 8.13 (s, 1H), 8.1 (s, 1H), 8.03 (s, 1H), 7.8 (s, 1H), 7–7.25 (m, 2H) $^{19}$F NMR: 128. Anal. calcd for $C_{10}H_8N_3F$: C, 63.49; H, 4.23; N, 22.22. Found: C, 63.28; H, 4.51; N, 22.09.

#### 5.1.23. Imidazo[1,5-*a*]quinoxaline-pyrazine-6-(5*H*)-one (15)

A mixture of **14** (7.50 g, 36 mmol) and sodium hydrure (1.1 g, 43 mmol) in dimethylacetamide (280 mL) was heated to reflux for 6 h. The reaction mixture was then concentrated under vacuum followed by the addition of water and saturated ammonium chloride. The solid was collected by filtration, washed with water, and dried to give 4 g of **15** (yield, 80%). $^1$H NMR (300 MHz, DMSO-$d_6$): $\delta$ 9.4 (s, 1H), 8.2 (d, 1H), 7.8 (d, 1H), 7.31 (d, 1H), 7.1-7.3 (m, 3H). Anal. calcd for $C_{10}H_7N_3O$: C, 64.86; H, 3.78; N, 22.70. Found: C, 65.11; H, 3.87; N, 22.93.

#### 5.1.24. 6-Chloroimidazo[1,5-*a*]quinoxaline (16)

**16** was prepared from **15** following the protocol described for **11**, that is, from **15** (4 g, 21.6 mmol) and phosphorus oxychloride (44 ml). The solid was collected by filtration and purified using column chromatography on silica gel to yield **16** as a yellow solid (yield, 20%). $^1$H NMR (300 MHz, DMSO-$d_6$): $\delta$ 9.4 (s, 1H), 8.2 (d, 1H), 7.8 (d, 1H), 7.31 (d, 1H), 7.1-7.3 (m, 3H). Anal. calcd for $C_{10}H_6N_3Cl$: C, 58.97; H, 2.95; N, 20.64. Found: C, 58.77; H, 2.72; N, 20.88.

#### 5.1.25. *N*-Methylimidazo[1,5-*a*]quinoxalin-4-amine (17a)

**17a** was prepared from **16** following the protocol described for **12a**, that is, from methylamine 2 × (0.25 mL of a 40% (w/v) aqueous solution, 2.7 mmol), **16** (0.11 g, 0.54 mmol), and EtOH (8 mL). The product was purified by column chromatography on silica gel with $C_6H_{12}$–EtOAc (70:30, v/v) as eluent to yield a cream solid (yield, 80–85%). Mp 255–258 °C. $^1$H NMR (300 MHz, DMSO-$d_6$): $\delta$ 8.54 (s, 1H), 7.75 (dd, $J_1$ = *1.33*, $J_2$ = *8.07*, 1H), 7,65 (dd, $J_1$ = *1.3*, $J_2$ = *8.11*, 1H), 7.59 (s, 1H), 7.35 (s, 1H), 7.25 (s, 1H), 3.24 (d, 3H).$^{13}$C NMR (300 MHz, DMSO-$d_6$): $\delta$ 147.50, 142.34, 135.54, 130.67, 129.16, 125.14, 124.34, 114.14, 111.24, 26.98. Anal. calcd for $C_{11}H_{10}N_4$: C, 66.65; H, 5.08; N, 28.26. Found: C, 66.54; H, 4.98; N, 28.15.

#### 5.1.26. *N*,*N*-Dimethylimidazo[1,5-*a*]quinoxalin-4-amine (17b)

**17b** was prepared from **16** following the protocol described for **17a**, that is, from dimethylamine (0.15 mL of a 40% (w/v) aqueous solution, 1.19 mmol), **16** (0.11 g, 0.54 mmol), and EtOH (10 mL). The product was purified by column chromatography on silica gel with $C_6H_{12}$–EtOAc (70:30, v/v) as eluent to give a white solid (yield, 96%). Mp 160–165°C. $^1$H NMR (300 MHz, DMSO-$d_6$): $\delta$ 8.55 (s, 1H), 7.78 (s, 1H), 7.71 (dd, $J_1$ = 1.25, $J_2$ = 8.07, 1H), 7.6 (dd, $J_1$ = 1.21, $J_2$ = 8.12, 1H), 7.35 (t, 1H), 7.15 (t, 1H), 3.43 (s, 6H). $^{13}$C NMR (300 MHz, DMSO-$d_6$): $\delta$ 146.93, 143.22, 135.50, 129.56, 129.08, 128.29, 125.48, 124.75, 114.49, 111.16, 37.89. Anal. Calcd for $C_{12}H_{12}N_4$: C, 67.91; H, 5.70; N, 26.40. Found: C, 67.64; H, 5.48; N, 26.53.

### 5.2. In vitro cytotoxic activity

#### 5.2.1. Materials and reagents

Imiquimod (Molekula, Wessex House, Shaftesbury, Dorset, UK), doxorubicin hydrochloride (Teva laboratory, Courbevoie, France),

fotemustine (Servier, Orléans, France), irinotecan (Aventis Pharma laboratories, Vitry-sur-Seine, France), methotrexate (Teva laboratory) were used in this study. 3-(4,5-Dimethylthiazol-2-yl)-2,5-diphenyltetrazolium bromide (MTT), isopropyl alcohol, and hydrochloric acid were obtained from Merck (Darmstadt, Germany). All other reagents were of analytical grade and were obtained from commercial sources.

#### 5.2.2. Cell lines and culture techniques

Melanoma (A375, M4Be and RPMI-7951), breath (MCF7), colon (LS174T), and B lymphoma (Raji) human cancer cell lines were obtained from American Type Culture Collection (Rockville, Md., USA). Cells were cultured in RPMI medium containing RPMI-1640 (Gibco Laboratories, France), with the exception of the M4Be line that required DMEM medium supplemented with 10% heat-inactived (56 °C) foetal bovine serum (FBS) (Polylabo, Paris, France), 2 mM L-glutamine, 100 IU/ml penicillin G sodium, 100 μg/ml streptomycin sulphate, and 0.25 μg/ml amphotericin B. Cells were maintained in a humidified atmosphere of 5% $CO_2$ in air at 37 °C.

#### 5.2.3. Cytotoxicity assay

Previously to the experiments, the number of cells by well, the doubling time and the MTT concentration have been optimized. In all the experiments, A375, M4Be, RPMI 7950, LS147T, MCF7, and Raji cells were seeded at a final concentration of 5000 cells/well in 96-well microtiter plates and allowed to attach overnight. After 20–24 h incubation, the medium was aspirated carefully from the plates using a sterile Pasteur pipette, and cells were exposed (i) to vehicle controls (1% DMSO/culture medium and culture medium alone), (ii) to doxorubicin, irinotecan, fotemustine, methotrexate, and imiquimod at concentrations of $10^{-4}$ to $10^{-10}$ μM, diluted in the culture medium, and (iii) to the synthesized compounds ($10^{-4}$–$10^{-10}$ μM) dissolved in a mixture 1% DMSO/culture medium (v/v). After 96 h of incubation, 10 μl of MTT solution in PBS (5 mg/ml, phosphate-buffer saline pH 7.3) was added to each well, and the wells were incubated at 37 °C for 4 h. This colorimetric assay is based on the ability of live and metabolically unimpaired tumor-cell targets to reduce MTT to a blue formazan product. At the end of the incubation period, the supernatant was carefully aspirated, then, 100 μl of a mixture of isopropyl alcohol and 1 M hydrochloric acid (96/4, v/v) was added to each well. After 10 min of incubation and vigorous shaking to solubilize formazan crystals, the optical density was measured at 570 nm in a microculture plate reader (Dynatech MR 5000, France). For each assay, at least three experiments were performed in triplicate.

The individual cell line growth curves confirmed that all tumor lines in control medium remained in the log phase of cell growth 96 h after plating. Cell survival was expressed as percent of vehicle control. The $IC_{50}$ values defined as the concentrations of drugs which produced 50% cell growth inhibition; 50% reduction of absorbance, were estimated from the sigmoidal dose–response curves.

#### 5.2.4. Xenografts and in vivo study protocol

This research adhered to the 'Principles of Laboratory Animal Care' (NIH publication #85-23, revised 1985). The animal study was approved by the local Animal Use Committee. Before to start pharmacodynamic studies in mouse, the 50% lethal dose ($LD_{50}$) of the **EAPB0203** compound was evaluated in healthy animal after intraperitoneal (ip) administration. The $LD_{50}$ was higher than 300 mg/kg.

M4Be tumor cells at logarithmic growth in vitro were harvested and washed twice with PBS. Tumor cells ($3 \times 10^6$) suspended in 150 μl of DMEM medium without FBS were inoculated subcutaneously into the flank area of female Swiss Nude mice (7 weeks old, weighing 20–22 g) through a 23-gauge needle. Mice were purchased from Charles River (L'Arbresle Cedex, France) and were kept under sterile conditions. They received sterile food and water. Tumor growth was monitored twice a week. Two perpendicular diameters (a and b) were measured with a Vernier caliper, and tumor volumes ($V$) were calculated using the following formula: $V = 0.5ab^2$ . At a tumor size of ~0.7 $cm^3$, athymic mice were randomized into three groups (6 mice per group): (i) the vehicle control group (weekly ip administration of DMSO/intralipid (50:50, v/v)), (ii) the **EAPB0203** group (two protocols: protocol 1, weekly ip administration of 5 mg/kg for 3 weeks and protocol 2, administration of 20 mg/kg twice a week (monday and thursday) for 3 weeks, this cycle was repeated after 15 days), and (iii) the fotemustine group (two protocols: protocol 1, weekly ip administration of 5 mg/kg for 3 weeks and protocol 2, weekly ip administration of 20 mg/kg for 3 weeks, this cycle was repeated after 15 days). **EAPB0203** being poorly soluble in water was dissolved in a mixture intralipid/DMSO (50:50, v/v). Fotemustine was dissolved in isotonic glucose. The dosing regimen of fotemustine is near to the fotemustine dose of 100 mg/$m^2$ used clinically. Animals were euthanized with $CO_2$ when the tumor size reached 2 $cm^3$.

Tumor response was assessed by comparing the tumor volume in each mouse group (control, fotemustine, and **EAPB0203**).

#### 5.2.5. Statistical analysis

In vivo results are presented as mean ± standard error of the mean (SEM). A one way ANOVA for repeated measurements was performed to compare (i) the efficacy of treatment according to the administered dose (5 and 20 mg/kg), both for fotemustine and **EAPB0203**; (ii) the variations of tumor volume between the three treatment groups (control, fotemustine, and **EAPB0203**) both at low and high administered doses. A simple contrast test was used to compare 2-by-2 each group; in this case, the level of significance was corrected for multiple comparisons and fixed at 0.02. This analysis was performed using the PK-fit software. Probability values of less than 0.05 were considered statistically significant.

## Acknowledgments

We thank Dr. Bompart Jacques for providing assistance in the chemistry part, Margout Delphine, Heintz Geneviève, Brissac Michel, and Imed Ait-Arsa for their precious technical support in the biological studies, and La Ligue contre le Cancer for its financial support.

## Supplementary data

Supplementary data associated with this article can be found, in the online version, at doi:10.1016/j.bmc.2008.05.022.

## References and notes

1. Rudy, S. J. *Dermatol. Nurs.* **2002**, *14*, 268–270.
2. Sidky, Y. A.; Borden, E. C.; Weeks, C. E.; Reiter, M. J.; Hatcher, J. F.; Bryan, G. T. *Cancer Res.* **1992**, *52*, 2528–2533.
3. Sauder, D. N. *Br. J. Dermatol.* **2003**, *149*, 5–8.
4. Reiter, M. J.; Testerman, T. L.; Miller, R. L.; Weeks, C. E.; Tomai, M. A. *J. Leukoc. Biol.* **1994**, *55*, 234–240.
5. Megyeri, K.; Au, W. C.; Rosztoczy, I.; Raj, N. B.; Miller, R. L.; Tomai, M. A.; Piha, P. M. *Mol. Cell. Biol.* **1995**, *15*, 2207–2218.
6. Steinmann, A.; Funk, J. O.; Schuler, G.; Von den Driech, P. *J. Am. Acad. Dermatol.* **2000**, *43*, 555–556.
7. Bong, A. B.; Bonnekoh, B.; Franke, I.; Schon, M. P.; Ulrich, J.; Gollnick, H. *J. Dermatol.* **2002**, *205*, 135–138.
8. Ugurel, S.; Wagner, A.; Phohler, C.; Tilgen, W.; Reinhold, U. *Br. J. Dermatol.* **2002**, *147*, 621–624.
9. Hengge, U. R.; Cusini, M. *Br. J. Dermatol.* **2003**, *149*, 15–19.
10. Spanner, D. E.; Miller, R. L.; Mena, J.; Crossman, L.; Sorrenti, V.; Ski, Y. *Leuk. Lymphoma* **2005**, *46*, 935–939.
11. Hemmi, H.; Kaisho, T.; Takeuchi, O.; Sato, S.; Sanjo, H.; Hoshimo, K.; Horiuchi, T.; Tomizawa, H.; Takeda, K.; Akira, S. *Nat. Immunol.* **2002**, *3*, 196–200.

12. Schon, M.; Bong, A. B.; Drewniok, C.; Herz, J.; Geilen, C. C.; Reifenberger, J.; Beinninghoff, B.; Slade, H. B.; Gollnick, H.; Schon, M. P. *J. Natl. Cancer Inst.* **2003**, *95*, 1138–1149.
13. Stockfeth, E.; Trefzer, U.; Gracia-Bartels, C.; Wegner, T.; Schmook, T.; Sterry, W. *Br. J. Dermatol.* **2003**, *149*, 53–56.
14. Schön, M. P.; Wienrich, B. G.; Drewniok, C.; Bong, A. B.; Eberle, J.; Geilen, C. C.; Gollnick, H.; Schön, M. *J. Invest. Dermatol.* **2004**, *122*, 1266–1276.
15. Deleuze-Masquefa, C.; Gerebtzoff, G.; Subra, G.; Fabreguettes, J. R.; Ovens, A.; Carraz, M.; Strub, M. P.; Bompart, J.; George, P.; Bonnet, P. A. *Bioorg. Med. Chem.* **2004**, *12*, 1129–1139.
16. Wagner, T. L.; Ahonen, C. L.; Couture, A. M.; Gibson, S. J.; Miller, R. L.; Smith, R. M. *Cell. Immunol.* **1999**, *191*, 10–19.
17. Gibson, S. J.; Imbertson, L. M.; Wagner, T. L. *J. Interferon Cytokine Res.* **1995**, *15*, 2207–2218.
18. Schön, M.; Bong, A. B.; Drewniok, C.; Herz, J.; Geilen, C. C.; Reifenberger, J.; Benninghoff, B.; Slade, H. B.; Gollnick, H.; Shön, M. P. *J. Natl. Cancer Inst.* **2003**, *95*, 1138–1149.
19. Morjarial, S.; Deleuze-Masquefa, C.; Lafont, V.; Gayraud, S.; Bompart, J.; Bonnet, P. A.; Dornand, J. *J. Immunopathol. Pharmacol.* **2006**, *19*, 525–538.
20. Chen, P.; Doweyko, A. M.; Norris, D.; Gu, H. H.; Spergel, S. H.; Das, J.; Moquin, M. V.; Lin, L.; Wityak, J.; Iwanowics, E. J. *J. Med. Chem.* **2004**, *47*, 4517–4529.
21. Moarbess, G.; El-Hajj, H.; Kfoury, Y.; El-Sabban, M. E.; Lepelletier, Y.; Hermine, O.; Deleuze-Masquéfa, C.; Bonnet, P. A.; Bazarbachi, A. *Blood* **2008**, *111*, 3770–3777.
22. Avril, M. F.; Aamdal, S.; Grob, J. J.; Hauschild, A.; Mohr, P.; Bonerandi, J. J.; Weichenthal, M.; Neuber, K.; Bieber, T.; Gilde, K.; Guillem Porta, V.; Fra, J.; Bonneterre, J.; Saïag, P.; Kamanabrou, D.; Pehamberger, H.; Sufliarsky, J.; Gonzalez Larriba, J. L.; Scherrer, A.; Menu, Y. *J. Clin. Oncol.* **2004**, *18*, 1118–1125.